Mechanical Confinement: An Effective Way of Tuning Properties of Piezoelectric Crystals

Mie Marsilius, Josh Frederick, Wei Hu, Xiaoli Tan, Torsten Granzow, and Pengdi Han*

Using <001>-oriented $Pb(Mg_{1/3}Nb_{2/3})O_3$–$PbTiO_3$ ferroelectric single crystals as a model material, the impact of mechanical confinements on polarization hysteresis, coercive field, and remanent polarization of relaxor-based piezocrystals is investigated. Comparative studies are made among rhombohedral and tetragonal single crystals, as well as a polycrystalline ceramic, under uniaxial and radial compressive pre-stresses. The dramatic changes observed are interpreted in terms of the piezoelectric effect and possible phase transitions for rhombohedral crystals, and ferroelastic domain switching and the piezoelectric effect for tetragonal crystals. Under radial compressive stresses, the coercive field for the rhombohedral crystal is observed to increase to 0.67 kV/mm and that for the tetragonal crystal is increased to 0.78 kV/mm. This is a 200% increase relative to the unstressed condition. The results demonstrate a general and effective approach to overcome the drawback of low coercive fields in these relaxor-based ferroelectric crystals, which could help facilitate widespread implementation of these piezocrystals in engineering devices.

1. Introduction

Relaxor-based ferroelectric single crystals, notably $Pb(Mg_{1/3}Nb_{2/3})O_3$–$PbTiO_3$ [PMN–PT] and $Pb(Zn_{1/3}Nb_{2/3})O_3$–$PbTiO_3$ [PZN–PT], have attracted significant attention over the last fifteen years.[1–10] Due to their ultrahigh piezoelectric properties, these single crystals are of great interest for many different electromechanical device applications.[3,10] The piezoelectric properties of these crystals vary markedly with the chemical composition in the vicinity of the morphotropic phase boundary (MPB), which separates a rhombohedral perovskite structure at low PT-content from a tetragonal perovskite at high PT-content.[7–9] Detailed structural analysis on the PMN–PT system reveals that the MPB spans from 30 to 38 mol.% of PT within which a monoclinic (M_C) phase coexists with the rhombohedral (30~32 mol.%) or the tetragonal (32~38 mol.%) phase.[9,11] The most remarkable properties are observed when the electric field is applied in the <001>-direction of a rhombohedral crystal.[2] This has been attributed to the rotation of the polarization vector from the pseudocubic <111> direction to the <001> direction, corresponding to an electric field-induced phase transition from the rhombohedral to the tetragonal via the intermediate monoclinic phase.[2,7–9]

Despite the excellent piezoelectric properties of these relaxor-based ferroelectric crystals, their widespread integration into engineering devices has been limited by their low Curie temperatures (T_c) and low coercive fields (E_c).[2,3,9] Typical values of E_c for PMN–PT and PZN–PT single crystals with MPB compositions are 0.2~0.3 kV/mm,[9] making them unsuitable for high-field applications. Currently the only way to overcome these disadvantages seems to be chemical modification. For example, E_c in the crystals of the MPB compositions in the $Pb(In_{1/2}Nb_{1/2})O_3$–$Pb(Mg_{1/3}Nb_{2/3})O_3$–$PbTiO_3$ ternary system can reach 0.6~0.7 kV/mm.[9,12,13] However, incorporating additional elements inevitably further complicates the crystal growth process and compromises the piezoelectric properties. Most importantly, indium is a scarce element in the earth's crust and its estimated reserves are extremely limited.[14] Since there exists evidence that the domain structure and electrical properties could be altered in PMN–PT single crystals[15–17] and polycrystalline ceramics[18,19] by application of external stresses, we speculate that mechanical confinement could be an alternative way to enhance E_c without sacrificing the piezoelectric coefficients in relaxor-based piezocrystals.

The present work systematically studies the effect of compressive stress on the ferroelectric hysteresis, coercive field and remanent polarization in <001>-oriented relaxor-based ferroelectric single crystals. PMN–PT single crystals with compositions on the rhombohedral and the tetragonal side of MPB are used as a model system. A special setup is utilized that allows the application of uniform radial compressive stresses to a cylindrical sample with electric fields applied along the cylinder axis.[20–22] The results are discussed with respect to polarization

J. Frederick, Dr. W. Hu, Prof. X. Tan
Department of Materials Science and Engineering
Iowa State University
Ames, IA 50011, USA
E-mail: xtan@iastate.edu
Dr. M. Marsilius, Dr. T. Granzow
Department of Materials Science
Technische Universität Darmstadt
64287 Darmstadt, Germany
Dr. P. D. Han
H.C. Materials Corporation
Bolingbrook, IL 60440, USA

DOI: 10.1002/adfm.201101301

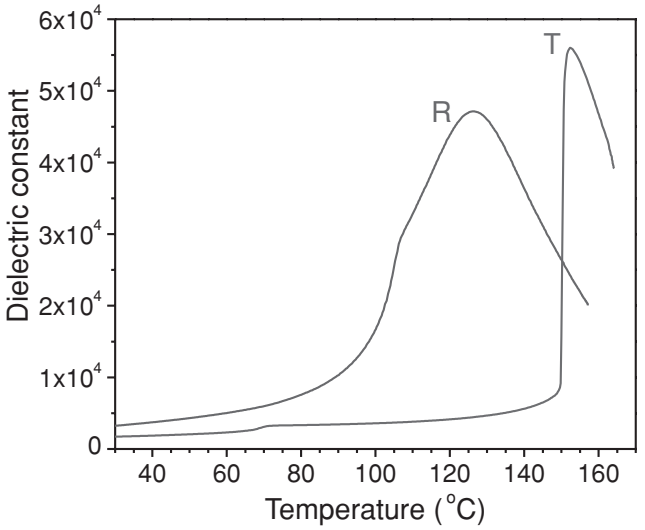

Figure 1. Dielectric constant vs. temperature for Crystal R and Crystal T measured at 1 kHz during heating at 3 °C/min.

reorientation and phase transition processes and contrasted to comparable measurements on a commercial soft lead zirconate titanate (PZT) ceramic.

2. Results

Due to the nature of the growth method, as-grown (1-x)PMN–xPT crystals inevitably possess composition segregations.[8,9] The exact composition of the crystal has been observed to correlate with its Curie temperature T_c according to the following empirical relation:

$$T_c = 500x - 10 \quad (1)$$

where T_c is in degrees centigrade and x is the content of PT.[8] The results of the dielectric measurement on the two PMN–PT crystals are shown in **Figure 1**. Upon heating at 3 °C per minute, T_c is measured to be 126 °C for one crystal and 152 °C for the other. Based on Equation (1), the PT content is 27.2 mol.% and 32.4 mol.%, respectively. According to the updated phase diagram shown in a previous report,[9] the crystal with 27.2 mol.% PT is in a pure rhombohedral phase at room temperature and is referred to as "Crystal R" in the present work. The anomaly at 106 °C corresponds to the rhombohedral to tetragonal phase transition. The other crystal is a mixture of monoclinic and tetragonal phases at room temperature and hence is noted as "Crystal T" hereafter. The anomaly at 68 °C marks the monoclinic to tetragonal phase transition during heating.

Figure 2 shows the polarization hysteresis loops of Crystal R under different levels of radial and uniaxial compressive stresses at room temperature. In **Figure 3**, the corresponding coercive field E_c and remanent polarization P_r are plotted versus stress to quantify the changes of the hysteresis curves. The error bars indicate the reproducibility of the measurement within a sample set of five test specimens. As shown in

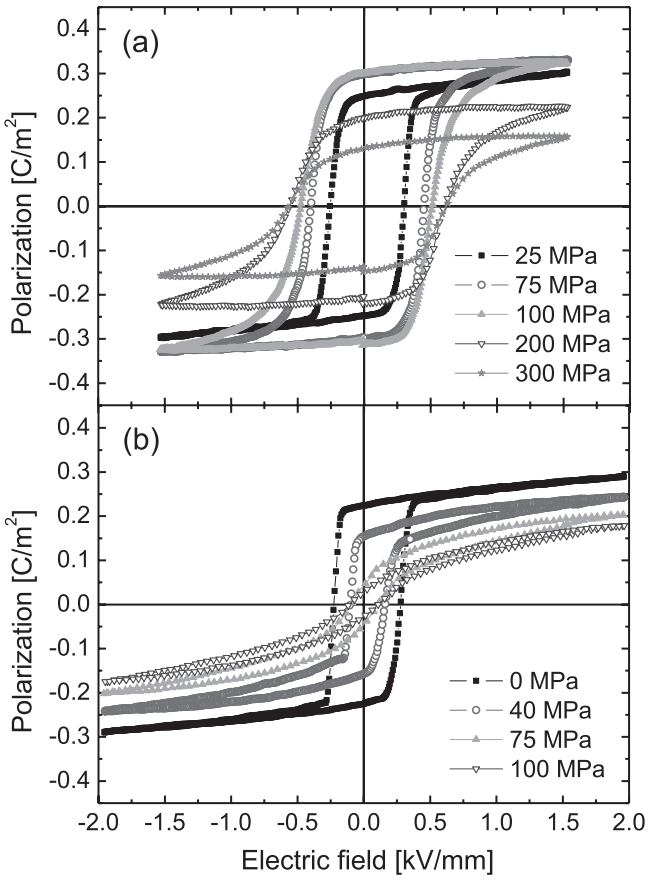

Figure 2. Polarization vs. electric field hysteresis loops recorded from Crystal R under different levels of a) radial, and b) uniaxial compressive confinements.

Figure 2a, increasing radial compressive stress leads to a broadening of the hysteresis curve. For low stress levels the main fraction of polarization reversal occurs within the immediate vicinity of the coercive field, leading to near-rectangular hysteresis loops. For higher stress levels the polarization change occurs in a broader field range, causing a smearing out of the loops. The dissipated energy, which is given by the area of the $P(E)$ loops, shows a maximum between 100 and 150 MPa. The coercive field under radial compression increases almost linearly up to a value of 0.67 kV/mm at 150 MPa and then stays constant above 150 MPa (Figure 3a). The remanent polarization increases for moderate radial stresses, exhibits a maximum of 0.3 C/m^2 at approximately 75 MPa and decreases nonlinearly above 100 MPa.

Applying an axial compressive stress parallel to the direction of the electric field reduces the hysteretic behavior and the dissipated energy significantly (Figure 2b). The smearing of the region of polarization reversal is even more pronounced than for radial stress application. The coercive field decreases linearly from 0.25 kV/mm at 0 MPa to 0.1 kV/mm at 50 MPa and stays almost constant above 50 MPa (Figure 3b). The remanent polarization continuously decreases over the whole investigated stress range from 0.23 C/m^2 for the stress-free state down to 0.03 C/m^2 at 100 MPa.

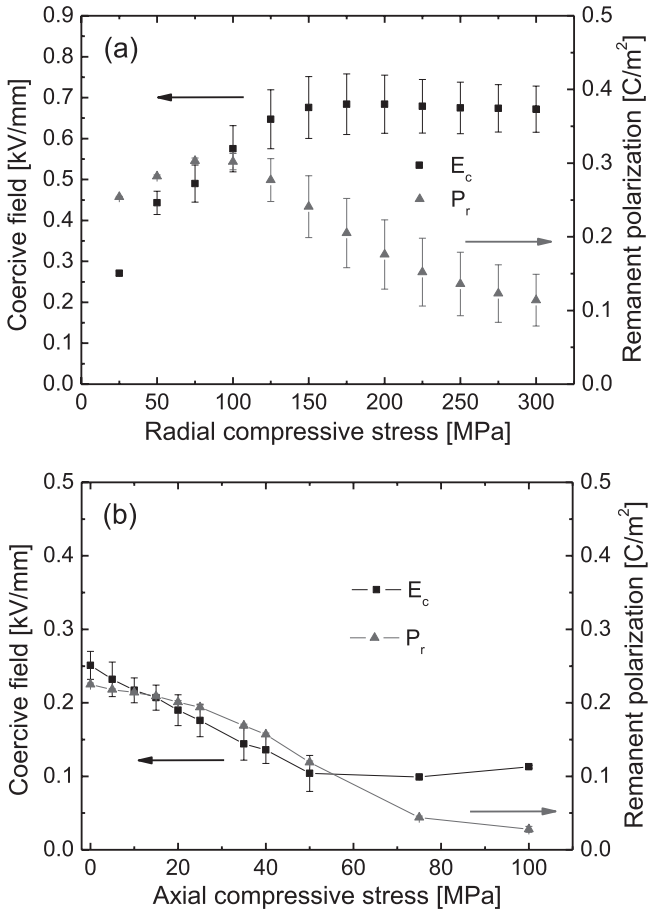

Figure 3. Remanent polarization P_r and coercive field E_c of Crystal R extracted from the hysteresis curves under a) radial, and b) uniaxial compressive pre-stresses.

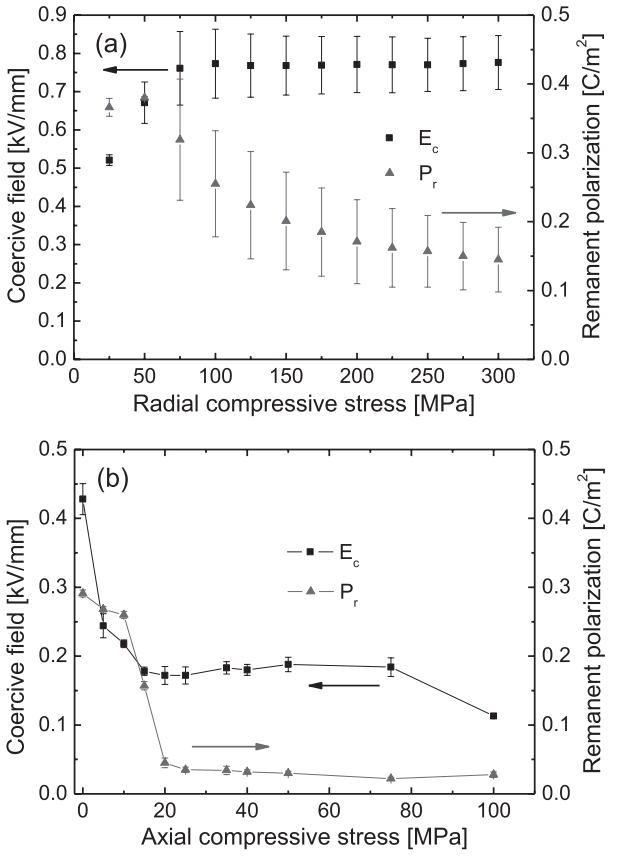

Figure 4. Remanent polarization P_r and coercive field E_c of Crystal T under a) radial, and b) uniaxial compressive pre-stresses.

The polarization hysteresis of Crystal T shows in principle a similar trend on external stresses as observed for Crystal R. **Figure 4** shows the coercive field and the remanent polarization of Crystal T as a function of the external compressive stress. The coercive field under the application of a radial load reaches its maximum value of 0.78 kV/mm at 75 MPa and stays constant for higher stress levels (Figure 4a). The remanent polarization exhibits a maximum of 0.38 C/m^2 at approximately 50 MPa before it decreases nonlinearly. Under the mechanical confinement of a uniaxial compression, the coercive field decreases very fast from a starting value of 0.43 kV/mm to 0.18 kV/mm at 15 MPa and plateaus at higher stress levels (Figure 4b). The remanent polarization shows a gradual decrease up to 10 MPa and abruptly vanishes at uniaxial compressive stresses of 20 MPa and above.

In **Figure 5**, the coercive field and remanent polarization of a polycrystalline PZT ceramic (PIC 151) under mechanical confinements are plotted. The data under the radial compressive stress (Figure 5a) are taken from a previous report.[21] It is apparent that the effect is almost negligible compared to that observed in PMN–PT single crystals. The coercive field varies by less than 10%, showing a maximum around 40 MPa. The remanent polarization increases slightly from 0.29 C/m^2 to 0.32 C/m^2 when the stress is increased from 0 to 100 MPa. In comparison, the uniaxial stress displays stronger influences on both the coercive field and the remanent polarization (Figure 5b). The relative changes are comparable to that observed in Crystal R, but not quite as pronounced as in Crystal T.

3. Discussion

To the authors' best knowledge, application of compressive stresses along a single direction that is perpendicular to the electric field direction or uniformly along all the radial directions to relaxor-based ferroelectric single crystals has not been attempted previously. Application of a uniaxial compressive stress in the direction of electric field to <001>-oriented PMN–PT piezocrystals reveals an increase in piezoelectric coefficient d_{33}[16,17] and a decrease in both E_c and P_r.[16] The experimental results in the present study indicate that the trend for the change of E_c and P_r with radial compression confinement is completely different from that with uniaxial compression. Under radial compressive stresses for both Crystal R and Crystal T, E_c initially increases significantly and then saturates, while P_r shows a continuous decrease after the initial increase. In contrast, under uniaxial compressive stresses, E_c and P_r decrease gradually in Crystal R and abruptly in Crystal T. Considering the very effective enhancement in both E_c (0.67 kV/mm for Crystal R, 0.78 kV/

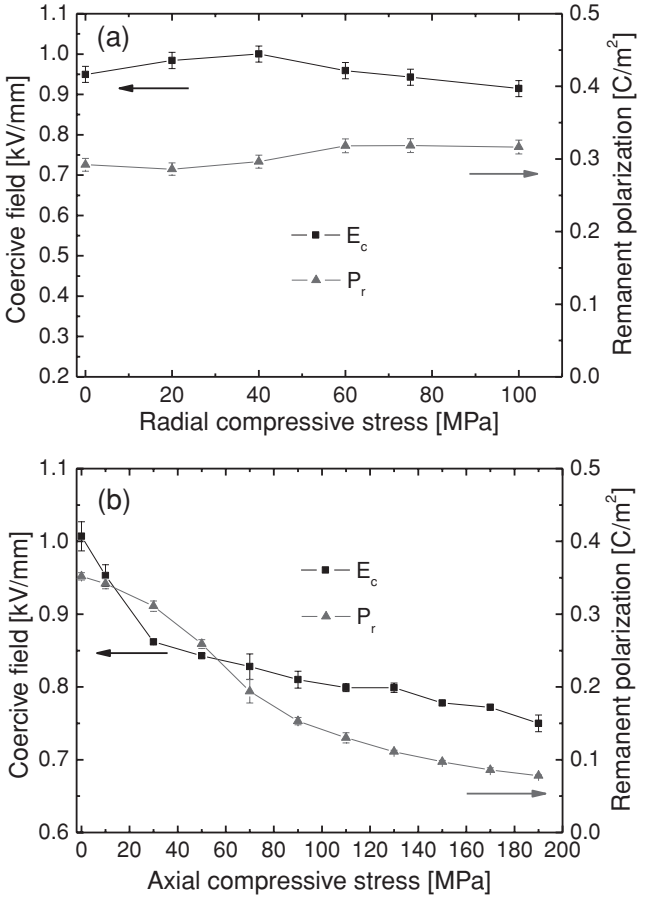

Figure 5. Remanent polarization P_r and coercive field E_c of a polycrystalline PZT ceramic with tetragonal symmetry under a) radial, and b) uniaxial compressive pre-stresses. The data in plot (a) are taken from Reference [21].

mm for Crystal T) and P_r, the present work demonstrates that radial mechanical confinement is an alternative way to enhance E_c without sacrificing the piezoelectric coefficients in relaxor-based piezocrystals.

To understand the changes in the ferroelectric properties under mechanical confinements observed here, the piezoelectric effect, ferroelectric- and ferroelastic-domain switching need to be considered. In the virgin state, Crystal R is in a pure rhombohedral phase at room temperature and the polar vectors in the unit cells are oriented in the <111> directions. After exposure to an external field directed along the [001] direction, ferroelectric domain variants of [111], [$\bar{1}$11], [1$\bar{1}$1] and [$\bar{1}\bar{1}$1] are expected. Thus a P_r that is lower than that of a tetragonal crystal is resulted. Although a mixture of monoclinic and tetragonal phases is expected in the virgin state of Crystal T, the exposure to an electric field in the [001] direction transforms the monoclinic phase to the tetragonal one. Therefore, the following discussion is made on the basis of a tetragonal crystal with polar vectors oriented in the <001> directions. Under combined mechanical and electric loadings applied in the present study, both 180°- and 90°-switching takes place and contributes to the measured polarization and strain. In addition, polarizations from compressive stresses or strains from electric fields through direct and converse piezoelectric effect are expected as well.

We first analyze the situation in Crystal R. The effects of mechanical loads on ferroelectric hysteresis behavior are usually attributed to non-180° ferroelectric/ferroelastic domain switching. In this respect, the results from Crystal R displayed in Figures 2 and 3 seem puzzling. All 8 variants of the <111> direction have the same projection of the spontaneous strain on the [001] axis. Therefore, neither radial nor axial mechanical loads in the present study should alter domain configurations in Crystal R. It should be noted here that additional measurements on Crystal R showed a small but detectable remanent strain of 0.04% after poling. In the ideal case when a rhombohedral crystal is poled along [001] direction, no remanent strain is expected. The observed remanent strain suggests that there might be slight miscut or growth defects in Crystal R. It is, however, by no means large enough to explain the remarkable hysteresis changes under stress.

We propose the piezoelectric effect (both direct and converse) is primarily responsible for the large change. Under radial pre-stresses, the direct piezoelectric effect contributes to an added polarization (and in turn to an increase in P_r) through

$$P_3 = d_{31} X_1 \tag{2}$$

where P_3 is the polarization along the poling direction, d_{31} is the transverse piezoelectric coefficient and X_1 represents the radial pre-stress. By fitting the data points of P_r at 25, 50, and 75 MPa in Figure 3a with Equation (2), a d_{31} of –980 pC/N is derived. This value matches very well with the reported values.[7,8] The increase in E_c seen in Figure 3a can be explained with assistance of the converse piezoelectric effect.

$$x_1 = d_{31} E_3 \tag{3}$$

If the applied electric field E_3 changes polarity (becomes negative), a positive transverse strain x_1 would result (the crystal would expand in radial directions) due to the negative d_{31}. However, this expansion is mechanically confined by the radial compressive pre-stress. As a result, polarization reversal becomes more and more difficult with increasing radial stress level. Figuratively speaking, the stress-induced deformation of the perovskite unit cell makes it difficult to pull the off-centered B-site cations through the (002) plane and reverse the polarization by a 180° switching process. Therefore, E_c increases. At the same time, this increase in E_c makes the domain switching incomplete under a fixed peak field (1.5 kV/mm) during test, which leads to an eventual decrease in P_r at radial stresses above 100 MPa. Another mechanism that cannot be ruled out is phase transition.[23–25] Under combined radial compressive stresses and electric fields, it is possible that Crystal R transforms toward a tetragonal phase through an intermediate monoclinic phase. The rotation of polar axis during this process explains the initial increase in P_r seen in Figure 3a.

Similar arguments can be applied to explain the response of Crystal R under the mechanical confinement of uniaxial compression along [001]. The direct piezoelectric effect ($P_3 = d_{33} X_3$) leads to a reduction of the polarization (X_3 is negative) in the loading direction. By fitting the data points

of P_r at X_3 up to 50 MPa in Figure 3(b), a d_{33} of 2010 pC/N is obtained. This value again matches very well with those in previous literature.[2,3,7–9] The polarization reversal process becomes easier for the same reason that radial compressive stresses make it harder. Under uniaxial compression, the elastic deformation produces a positive transverse strain, which is in synergy with the transverse expansion resulted from the converse piezoelectric effect described by Equation (3). In other words, the mechanical confinement under this configuration assists the electric field-driven domain polarization reversal. As a result, E_c decreases. Again, there are possibilities that phase transitions take place and make contributions to the observed changes. The compressive pre-stress could transform the rhombohedral phase to either an orthorhombic[23] or a tetragonal[24] phase, with polarization vectors perpendicular to the mechanical loading axis. The transformed regions in Crystal R then do not contribute to the polarization measured in the field direction, resulting in the observed decrease of P_r. Additionally, new pathways open for polarization reversal: a multi-step process via intermediate states in the orthorhombic/tetragonal phases, which could make domain switching easier and reduce E_c.

We now analyze the situation in Crystal T. Compared to Crystal R, the difference is that ferroelastic domain switching takes place and phase transition is not likely to occur. Under radial pre-stresses, polar vectors will be aligned along the electric field direction through 90° ferroelastic domain switching. As a result, ferroelectric domain switching under electric fields occurs only through 180° reversal. Similar to the situation in Crystal R, the initial increase in P_r is attributed to the direct piezoelectric effect described by Equation (2), while the increase in E_c is due to the fact that the radial mechanical confinement acts against the converse piezoelectric effect. Further increase in E_c reduces the volume fraction of switchable domains under a fixed peak field (1.5 kV/mm) during testing, leading to the decrease in P_r at higher stress levels.

When Crystal T is subjected to uniaxial compressive pre-stresses, ferroelastic domain switching turns the polar vector 90° away from the electric field direction. It was reported before that 90° ferroelastic domain switching took place at uniaxial compressive stresses around 20 MPa.[17] This explains the abrupt drop in P_r at 15 and 20 MPa seen in Figure 4b. To elucidate the counteracting ferroelectric and ferroelastic 90° domain switching process, the polarization hysteresis loop at 15 MPa is shown in **Figure 6**. Under the compressive pre-stress of 15 MPa and at electric fields of up to E_c (0.18 kV/mm in Figure 6), the polar vectors of most domains in Crystal T are in the transverse direction. During the loading process with electric field above E_c, positive polarization starts to appear as a result of the electric field-induced 90° ferroelectric domain switching. This switching is also the reverse 90° ferroelastic domain switching. When the electric field is below E_c (0.18 kV/mm) during unloading, the uniaxial pre-stress takes over and ferroelastic domain switching reduces the polarization dramatically by turning polar vectors to perpendicular directions. As a result, a double-loop behavior is seen in Figure 6. When the uniaxial pre-stresses are at 20 MPa and above, the applied electric field becomes incapable of inducing any ferroelectric domain switching. Crystal T then behaves like a linear dielectric and the values of P_r and E_c do not have any physical significance. At 5 MPa and 10 MPa pre-stresses, ferroelastic domain switching has not been triggered. The moderate decrease in P_r at these stress levels shown in Figure 4b is due to the direct piezoelectric effect. The reduction in E_c is attributed to the cooperative elastic deformation and converse piezoelectric effect. It is interesting to note that the transition from ferroelectric to antiferroelectric-like, then to paraelectric-like behavior in Crystal T under increasing uniaxial compressive stresses at room temperature resembles very closely the evolution of hysteresis loops with temperature in Sn-modified $Pb(Zr,Ti)O_3$ and $(Bi_{1/2}Na_{1/2})TiO_3$-based compositions.[26–28]

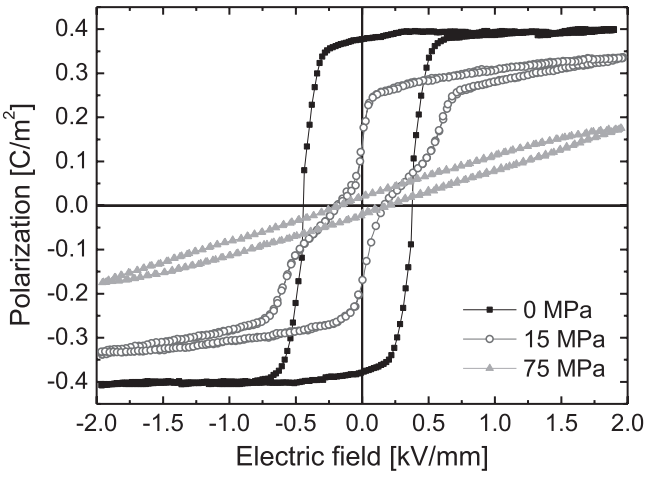

Figure 6. Polarization vs. electric field hysteresis loops recorded from Crystal T under three representative levels of uniaxial compressive pre-stress.

It is instructive to compare the data for the PMN–PT single crystals to that obtained in similar measurements on a polycrystalline PZT ceramic (Figure 5). It is remarkable that the influence of the radial compressive pre-stress is nearly negligible in the ceramic compared to both single crystals. The most plausible reason for the weak effect is the comparatively low piezoelectric coefficients in the PZT ceramic. Though less likely, the lower pre-stress level (100 MPa for ceramic vs. 300 MPa for crystals) could also be a factor. Under uniaxial pre-stresses, the behavior of the ceramic is much more similar to that of Crystal R, even though the ceramic is of tetragonal symmetry. In a simple way, this can be explained by the random orientation of individual grains in the ceramic. The polar vectors of the domains within the grains can be tilted at any angles relative to the electric field direction. The situation is comparable to that in Crystal R where polar vectors are along all 8 equivalent <111> directions.

4. Conclusions

Uniaxial compressive pre-stresses suppress the polarization hysteresis, leading to a lower coercive field and remanent polarization, for both Crystal R and Crystal T. In contrast,

radial compressive pre-stresses broaden the hysteresis loops for both crystals. With increasing pre-stress levels, the coercive field increases dramatically (up to a 200% increase) and then saturates, while the remanent polarization initially increases and then decreases. The observed changes in coercive field and remanent polarization as a function of the pre-stress level can be explained by the direct/converse piezoelectric effect and possible phase transitions in Crystal R and by the ferroelastic domain switching and direct/converse piezoelectric effect in Crystal T. Most importantly, the present experimental study establishes an effective way to increase the coercive field, which could potentially lead to new applications of these piezocrystals in high-field and high-power devices.

5. Experimental Section

Large PMN–PT single crystals were grown with the modified Bridgeman method. Crystals with compositions close to the morphotropic phase boundary were used for this study. Dielectric constant measurement was carried out on (001) thin crystals during heating at 3 °C/min. Prior to that, the thin crystals were annealed at 200 °C for 10 minutes. For hysteresis measurements under radial pre-stresses, specimens were prepared in a cylindrical geometry with 6 mm in diameter and 4~5 mm in height. For measurements under uniaxial pre-stresses, disk shaped specimens with 7 mm in diameter and 1 mm in thickness were used. In both specimen geometries regardless of the crystal symmetry (Crystal R or T), the pseudocubic <100>-direction was perpendicular to the circular faces along the cylindrical axis. The two circular faces were lapped and polished to ensure even, coplanar surfaces and to avoid electrical breakdown. They were sputtered with a layer of Ag approximately 90 nm in thickness. For all the hysteresis measurements, the electric field was always applied along the cylindrical axis, i.e., the pseudocubic <100>-direction. This direction is referred to as the poling direction in the text.

For radial compressive pre-stress tests, the specimens were loaded into a tube-like polyethylene fixture which fits tightly into a stiff steel housing. Using a hydraulic mechanical testing setup, an axial pressure was applied to the polyethylene tube leading to a radial compressive stress on the sample.[20] The *P–E* hysteresis loops under uniaxial compressive pre-stresses were measured using a 10 kN load frame while the specimen was held in place by a custom-built alignment fixture.[29] The stress level was increased stepwise up to 300 MPa (100 MPa) for the radial (axial) pre-stress, respectively. On each step the pre-stress was maintained constant while a bipolar electric field with a triangular waveform at a frequency of 105 mHz was applied. The polarization hysteresis was then recorded using a Sawyer-Tower circuit. For comparison, the measurements under uniaxial pre-stresses were also carried out on PIC 151 (PI Ceramics, Lederhose, Germany), a co-doped soft PZT polycrystalline ceramic with a composition on the tetragonal side of the morphotropic phase boundary.

Acknowledgements

This work was supported by the National Science Foundation (NSF) through Grant CMMI-1027873 and the Deutsche Forschungsgemeinschaft (DFG) under GR 2722/4-2.

Received: June 8, 2011
Revised: August 17, 2011
Published online: December 16, 2011

[1] J. Kuwata, K. Uchino, S. Nomura, *Jpn. J. Appl. Phys.* **1982**, *21*, 1298.
[2] S. E. Park, T. R. Shrout, *J. Appl. Phys.* **1997**, *82*, 1804.
[3] S. E. Park, T. R. Shrout, *IEEE Trans. Ultrason. Ferroelect. Freq. Contr.* **1997**, *44*, 1140.
[4] X. Tan, Z. Xu, J. K. Shang, P. Han, *Appl. Phys. Lett.* **2000**, *77*, 1529.
[5] B. J. Fang, Y. J. Shan, H. Q. Xu, H. S. Luo, Z. W. Yin, *Adv. Funct. Mater.* **2004**, *14*, 169.
[6] X. Zhao, W. Qu, X. Tan, A. Bokov, Z. G. Ye, *Phys. Rev. B* **2007**, *75*, 104106.
[7] Y. P. Guo, H. S. Luo, D. Ling, H. Q. Xu, T. H. He, Z. W. Yin, *J. Phys.: Condens. Matter* **2003**, *15*, L77.
[8] X. B. Li, H. S. Luo, *J. Am. Ceram. Soc.* **2010**, *93*, 2915.
[9] Z. G. Ye, *MRS Bullet.* **2009**, *34*, 277.
[10] H. J. Lee, S. J. Zhang, J. Luo, F. Li, T. R. Shrout, *Adv. Funct. Mater.* **2010**, *20*, 3154.
[11] B. Noheda, D. E. Cox, G. Shirane, J. Gao, Z. G. Ye, *Phys. Rev. B* **2002**, *66*, 054104.
[12] Y. Hosono, Y. Yamashita, H. Sakamoto, N. Ichinose, *Jpn. J. Appl. Phys.* **2003**, *42*, 5681.
[13] J. Tian, P. D. Han, X. L. Huang, H. X. Pan, J. F. Carroll, D. A. Payne, *Appl. Phys. Lett.* **2007**, *91*, 222903.
[14] T. J. Coutts, D. L. Young, X. Li, W. P. Mulligan, X. Wu, *J. Vac. Sci. Technol. A* **2000**, *18*, 2646.
[15] J. K. Shang, X. Tan, *Acta Mater.* **2001**, *49*, 2993.
[16] Q. Wan, C. Chen, Y. P. Shen, *J. Appl. Phys.* **2005**, *98*, 024103.
[17] D. Viehland, *J. Am. Ceram. Soc.* **2006**, *89*, 775.
[18] J. Zhao, A. E. Glazounov, Q. M. Zhang, *Appl. Phys. Lett.* **1999**, *74*, 436.
[19] M. Unruan, A. Ngamjarurojana, Y. Laosiritaworn, S. Ananta, R. Yimnirun, *J. Appl. Phys.* **2008**, *104*, 034101.
[20] T. Granzow, A. B. Kounga, E. Aulbach, J. Rödel, *Appl. Phys. Lett.* **2006**, *88*, 252907.
[21] T. Granzow, T. Leist, A. B. Kounga, E. Aulbach, J. Rödel, *Appl. Phys. Lett.* **2007**, *91*, 142904.
[22] X. Tan, J. Frederick, C. Ma, E. Aulbach, M. Marsilius, W. Hong, T. Granzow, W. Jo, J. Rödel, *Phys. Rev. B* **2010**, *81*, 014103.
[23] E. A. McLaughlin, T. Q. Liu, C. S. Lynch, *Acta Mater.* **2005**, *53*, 4001.
[24] K. G. Webber, R. Zuo, C. S. Lynch, *Acta Mater.* **2008**, *56*, 1219.
[25] M. Shanthi, L. C. Lim, *Appl. Phys. Lett.* **2009**, *95*, 102901.
[26] D. Viehland, D. Forst, Z. Xu, J. F. Li, *J. Am. Ceram. Soc.* **1995**, *78*, 2101.
[27] J. Frederick, X. Tan, W. Jo, *J. Am. Ceram. Soc.* **2011**, *94*, 1149.
[28] C. Xu, D. Lin, K. W. Kwok, *Solid State Sci.* **2008**, *10*, 934.
[29] X. Tan, E. Aulbach, W. Jo, T. Granzow, J. Kling, M. Marsilius, H. J. Kleebe, J. Rödel, *J. Appl. Phys.* **2009**, *106*, 044107.